International Journal of Power Electronics and Drive System (IJPEDS)
Vol. 17, No. 1, March 2026, pp. 425~437
ISSN: 2088-8694, DOI: 10.11591/ijpeds.v17.i1.pp425-437

D-STATCOM control for distribution grids with distributed sources based on MMC structure using FCS-MPC algorithm

Pham Viet Phuong[1], Le Hoai Nam[1], Pham Chi Hieu[1], Tran Hung Cuong[2]
[1]Department of Automation Engineering, School of Electrical and Electronic Engineering, Hanoi University of Science and Technology, Hanoi, Vietnam
[2]Faculty of Electrical and Electronic Engineering, Phenikaa University, Hanoi, Vietnam

Article Info

Article history:

Received Jul 24, 2025
Revised Feb 4, 2026
Accepted Feb 15, 2026

Keywords:

Distributed static synchronous compensator
Finite control set
Model predictive control
Modular multilevel converter
Reactive power compensation

ABSTRACT

This paper proposes a D-STATCOM structure based on a modular multilevel converter (MMC) with the use of FCS-MPC control method for the purpose of compensating reactive power and stabilizing voltage in the distribution grid. The D-STATCOM is effectively used in cases involving non-sinusoidal and unstable voltages, which often occur in the distribution grid due to the effects of unbalanced nonlinear loads and power injection from renewable energy systems. The proposed structure also has the capability of reactive power compensating flexibility in fault conditions to stabilize the grid voltage. In this paper, a new control strategy, which is based on the combination of an outer PI controller and an inner FCS-MPC controller, was introduced. The outer PI controller is used to reduce static deviations in control values and to provide a reference value for the FCS-MPC controller. The inner FCS-MPC controller calculates the optimal switching state for the purpose of reducing the switching frequency of the MMC. The implementation process begins with the construction of a mathematical model and a control model. Simulations were carried out by MATLAB/Simulink to demonstrate the responsiveness of the control algorithm and the performance of D-STATCOM under the conditions of non-sinusoidal and unstable voltages.

Corresponding Author:

Tran Hung Cuong
Faculty of Electrical and Electronic Engineering, Phenikaa University
Duong Noi, Hanoi 12116, Vietnam
Email: cuong.tranhung@phenikaa-uni.edu.vn

1. INTRODUCTION

The power quality of the distribution grid can be reduced in several cases, such as: i) The presence of nonlinear elements; and ii) The integration of renewable energy sources. In these cases, the voltage of the distribution grid becomes non-sinusoidal and distorted. As a result, the reactive power required for the loads may be insufficient, leading to unstable and inefficient operation of the electrical equipment [1]-[5]. In a standard distribution grid, these problems were typically solved by using the conventional compensation equipment located at the transformer station, as presented in documents [6], [7]. However, in modern distribution grids where renewable energy sources such as PVs and wind turbines are integrated, significant fluctuations in power components will occur due to the variations in voltage and uncontrollable current [8]-[10]. In these cases, the normal operation of the electrical equipment that consumes energy from the grid will be affected. The D-STATCOM has recently become an excellent piece of equipment to compensate for the insufficient reactive power as well as to regulate the voltage of the distribution grid; its importance is presented in document [11]. Compared with conventional static capacitor and Thyristor technology-based

compensation devices, D-STATCOM has many outstanding advantages in its operation, such as: instantaneous compensation response and the ability to compensate large amounts of power flexibly [12]-[15]. These advantages come from the use of three-phase voltage source converter such as NPC and CHB, in D-STATCOM's structure. However, in some operating conditions, such as unbalanced loads and asymmetrical voltage sources, the D-STATCOM faces some limitations [16]. These advantages come from the use of three-phase voltage source converter such as NPC and CHB, in D-STATCOM's structure. However, in some operating conditions, such as unbalanced loads and asymmetrical voltage sources, the D-STATCOM faces some limitations, as in document [16]. This paper proposes a D-STATCOM structure using a modular multilevel converter MMC together with module predictive control MPC method for reactive power compensation with the aim of stabilizing voltage, improving power factor, and providing sufficient reactive power required by the grid. The control system consists of an outer PI controller and an inner FCS-MPC controller. The outer PI controller is used to reduce static deviations in control values and to provide a reference value for the FCS-MPC controller, while the inner FCS-MPC controller calculates the optimal switching state for the purpose of reducing the switching frequency of the MMC. Simulations were carried out by MATLAB/Simulink to demonstrate the responsiveness of the control algorithm and the performance of D-STATCOM under the conditions of non-sinusoidal and unstable voltages.

2. D-STATCOM MODEL BASED ON MMC STRUCTURE

2.1. D-STATCOM structure based on MMC converters

Figure 1 shows the circuit diagram of an MMC-based D-STATCOM for the purpose of reactive power exchange with the power system. In Figure 1, each phase of the MMC converter consists of 2N SMs divided equally into two valve branches. The MMC converter uses only one dc source voltage at the input to generate an ac multilevel voltage at the output side. Theoretically, the ac voltage of the MMC converter can be expanded to an unlimited level by increasing the number of sub-modules (SMs) in each phase of the converter. As a result, the transformer as well as the ac filters are not required at the ac side of the MMC converter [17], [18]. Each sub-module of the MMC converter consists of two IGBTs, S1 and S2, as shown in Figure 1, to establish a half-bridge DC–AC converter. The output voltage of the MMC is obtained by "inserted" or "bypassed" states of the SMs in each phase of the converter. When the current has the positive direction as shown in Figures 2(a) and 2(b) or has the negative direction as shown in Figures 2(c) and 2(d), the "inserted" state can be obtained when S1 is ON and S2 is OFF producing a voltage of VSM = VC = VDC/N at the AC side of SM while the "bypassed" state can be obtained when S1 is OFF and S2 is ON producing a voltage of VSM = 0 at the AC side of SM.

2.2. Operating principle of the D-STATCOM

The Distributed Static Synchronous Compensator (D-STATCOM) is a voltage source converter (VSC) designed to operate as a solid-state synchronous voltage source shunt connected to AC transmission lines for dynamic compensation and real-time control [19]. Figure 1 shows the equivalent circuit of the D-STATCOM, in which the active and reactive powers exchanged at the PCC theoretically can be calculated as shown in (1).

$$P_1 = \frac{V_1 V_2 \sin\delta}{X_L}; Q_1 = \frac{V_1(V_1 - V_2\cos\delta)}{X_L} \quad (1)$$

In this equation, V1 and V2 represent the amplitudes of the voltages at the grid and converter sides, respectively. The variable δ is the phase difference between V1 and V2, while XL is the equivalent reactance connecting the grid and the converter. D-STATCOM is one of the FACTs devices that supports reactive power exchange with the power grid. (1) shows that V1 and V2 must be in phase, meaning δ = 0, allowing for reactive power exchange at the PCC by controlling the amplitudes of V1 and V2. As a result, (1) can be rewritten as in (2).

$$P_1 = 0; Q_1 = \frac{V_1(V_1 - V_2)}{X_L} \quad (2)$$

Figure 3 shows the operating principle of the D-STATCOM for the purpose of reactive power exchange. When V1 > V2, the reactive power Q in (2) is positive, resulting in the presence of a voltage component V12 as shown in Figure 3(a). In this case, the D-STATCOM operates in the inductive current mode with the inductive current IL being π/2 out of phase with V1 and V2. The D-STATCOM absorbs reactive power from the power grid. When V1 < V2, the reactive power Q in (2) is negative, resulting in the presence of a voltage component V12 as shown in Figure 3(b). In this case, the D-STATCOM operates in the

capacitive current mode with the capacitive current IC being π/2 out of phase with V1 and V2. The D-STATCOM releases the reactive power to the power grid. When V1 = V2 as shown in Figure 3(c), the D-STATCOM does not exchange the reactive power with the power grid.

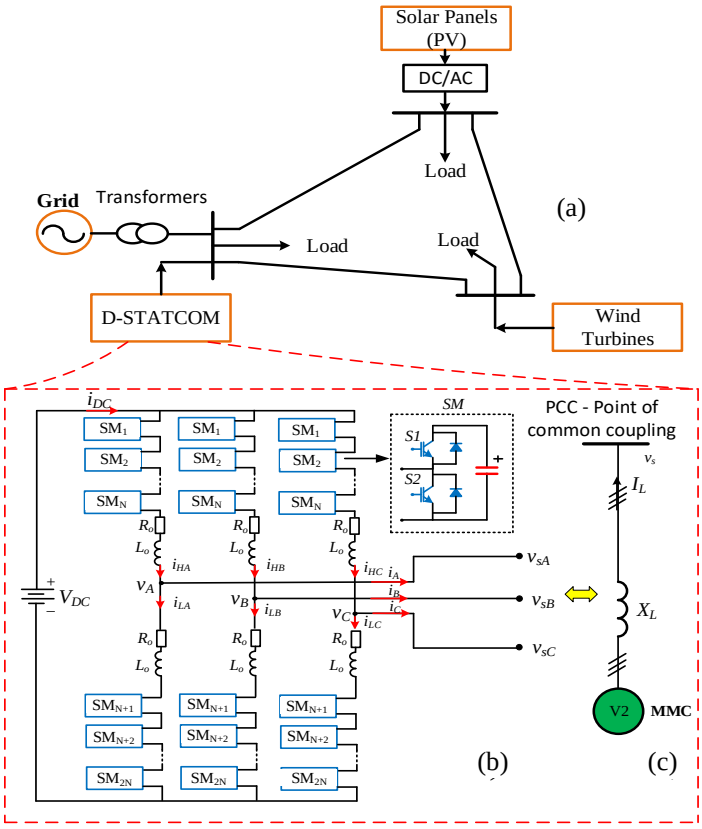

Figure 1. Schematic diagram of a grid connected MMC-based D-STATCOM

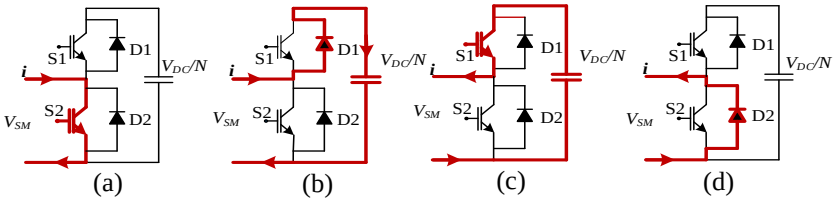

Figure 2. Switching operations of SM: (a) bypass with positive current, (b) insert with positive current, (c) insert with negative current, and (d) bypass with negative current

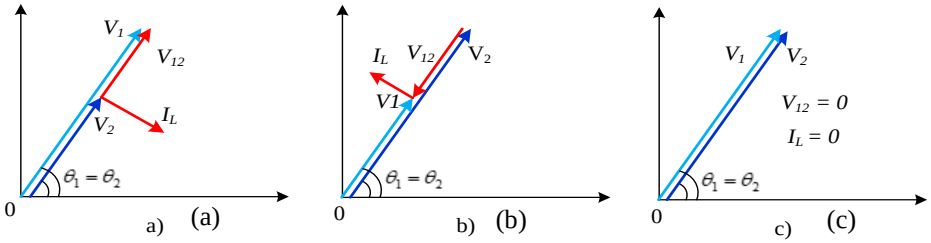

Figure 3. Operating principles of D-STATCOM: (a) state of reactive power absorption, (b) state of reactive power generation, and (c) state of no reactive power exchange

3. CONTROL SYSTEM FOR D-STATCOM

3.1. Math model of the MMC

The grid-connected MMC is shown in Figure 4. In this configuration, the MMC has three phases with six valve arms, each valve arm is divided into two parts, an upper arm and a lower arm, and in each arm there are N identical SMs connected in series. SMs are series connected with one inductor (L_o) and one resistor (R_o). The inductor L_o limits the short-circuit current of an MMC and removes the high-frequency harmonics of the current arm [20]. The resistor R_o represents the power losses within each arm.

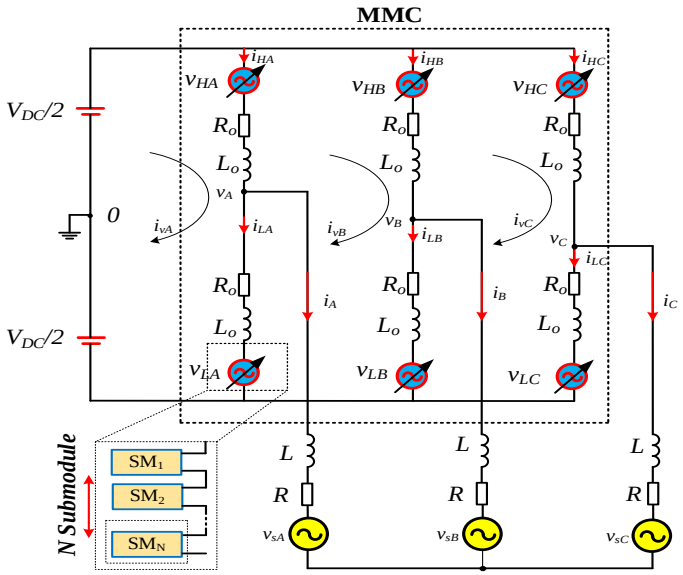

Figure 4. Structure the three-phase of the MMC on the DC/AC side

The SM's configuration is a half-bridge converter with the operating mode shown in Figure 2. During operation, each SM provides an output voltage of 0 or vC based on the states of S1 and S2. Specifically, Figure 2(a) shows the output voltage of the SM as vC, at which point S1 = ON and S2 = OFF. Figure 2(c) shows the output voltage of the SM as 0, at which point S1 = OFF and S2 = ON. These SMs operate based on control commands from the microprocessor system. In one operating cycle, the microprocessor commands always ensure that only N SMs are switched on (with an output voltage of vC) to create a stepped voltage of N+1 at the output of the MMC. Based on the laws of current, the mathematical equations describing the operation of phase x (x = A, B, C) in the MMC are represented as (3)-(5).

$$\frac{V_{DC}}{2} - v_{Hx} - Ri_{Hx} - L\frac{di_{Hx}}{dt} + R_o i_x + L_o \frac{di_x}{dt} - v_x = 0 \quad (3)$$

$$-\frac{V_{DC}}{2} + v_{Lx} + Ri_{Lx} + L\frac{di_{Lx}}{dt} + R_o i_x + L_o \frac{di_x}{dt} - v_x = 0 \quad (4)$$

$$i_{Hx} = \frac{-i_x}{2} + i_{vx}; i_{Lx} = \frac{i_x}{2} + i_{vx} \quad (5)$$

Where: i_{Hx} and i_{Lx} are the currents in each arm (upper arm and lower arm); i_{vx} is the circulating current in each phase. i_{vx} does not affect the quality of the alternating current, but i_{vx} will cause power loss inside the MMC [21]. Therefore, when the MMC is working, it is desirable that i_{vx} always has the smallest value; this is difficult to achieve by conventional means. The circulating current in the circuit in (6).

$$i_{vx} = \frac{i_{Hx}+i_{Lx}}{2} \quad (6)$$

By calculating based on (3)-(6), we can deduce (7) and (8), which represent the phase current and loop current in the circuit.

$$\frac{di_x}{dt} = \frac{-(R+2R_o)}{L+2L_o} i_x + \frac{v_{Hx}-v_{Lx}}{L+2L_o} + \frac{2v_x}{L+2L_o} \quad (7)$$

$$\frac{di_{vx}}{dt} = \frac{-R}{L} i_{vx} - \frac{1}{2L}(v_{Hx} + v_{Lx}) + \frac{1}{2L} V_{DC} \quad (8)$$

When inserting or omitting SMs according to the control law, a voltage is generated on each branch. The specific number of SMs inserted for the upper and lower branches based on the control law will be n_{Hx} and $n_{Lx,}$ respectively, and the corresponding voltage values generated in this case are v_{Hx} and v_{Lx}. When the control law affects the SMs to change the number of SMs, the capacitor voltage value of the SMs changes depending on the direction of the current in each branch. When the voltages on the capacitors are balanced, the voltage on each capacitor is approximately equal to v_{mx}/N $(m = H, L)$, where v_{mx} is the total capacitor voltage of each valve branch. Then, the branch voltage is expressed by (9).

$$v_{mx} = \frac{n_{mx} v_{mx}}{N} \quad (9)$$

Expresses a total capacitor (10):

$$\frac{dv_{mx}}{dt} = \frac{i_{mx}}{C_{mx}} = \frac{n_{mx} i_{mx}}{C} \quad (10)$$

Here, the value of the capacitor in one working cycle is C_m. When replacing i_{Hx} and i_{Lx} from (5), (6) into (10), we can deduce the equation relating the capacitor voltage on each branch, along with the number of SM inserted and the current $i_{vx,}$ as (11) and (12).

$$\frac{dv_{Hx}}{dt} = -\frac{n_{Hx}}{2C} i_{vx} + \frac{n_{Hx}}{C} i_{vx} \quad (11)$$

$$\frac{dv_{Lx}}{dt} = \frac{n_{Lx}}{2C} i_{vx} + \frac{n_{Lx}}{C} i_{vx} \quad (12)$$

3.2. The operating principle of MMC is based on the FCS-MPC control algorithm

This section will present the operation of the MMC based on the FCS-MPC control algorithm. The process is performed based on predicting the AC current value of the MMC at a future time according to the model at the present time. Then, optimize the cost function to select the best valve on/off state in one operating cycle of the MMC. To do this, the first step is to construct a discrete-time model to predict one step forward of the controllable variables of the MMC converter. Next is establishes a cost function associated with a predefined control objective. Finally, evaluate the cost function for all switching states in one cycle of the MMC, thereby selecting the optimal switching state in terms of quality for the alternating current of the MMC. The steps are shown in Figure 5(a) [22]. In which i(k) is the control variable, i(k+1) is the predicted value of i(k) in the next cycle, iref(k+1) is the reference value of i(k+1), S(k) are the optimized IGBT valve on/off states. The current control process by the FCS-MPC strategy is shown in detail in Figure 5(b). In there, the output AC current will be controlled closely to the reference value. According to [13], in a single-phase (n+1) level MMC, the total possible switching states are:

$$N = C_{2n}^{n} = \frac{2n!}{n!(2n-n)!} \quad (13)$$

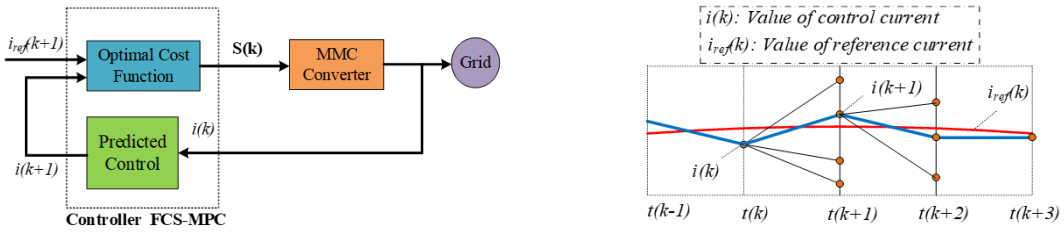

Figure 5. MPC controller for MMC: (a) MPC control method structure for MMC and (b) algorithm of predictive control for current AC

From (13), we can deduce that in the three phases of the MMC, there will be N^3 switching states. The FCS-MPC control process will calculate the cost function to determine the optimal switching state at a future time to apply to the MMC. To do this, (12) must be discretized using the Euler method. Assuming the

sampling period of the system is T_s, when discretizing (12), we get the discrete-time model of the MMC output current as (14).

$$i_x(k+1) = M.i_x(k) + N.[v_{xH}(k+1) - v_{xH}(k+1) - 2v_{Cx}(k+1).P] \quad (14)$$

In which:

$$v_{xm}(k+1) = \frac{1}{6}\sum_{x=A,B,C}\left(v_{Lx}(k+1) - v_{Hx}(k+1)\right); M = \frac{L_o+2L-T_S(R_o+2R)}{L_o+2L};\ N = \frac{T_S}{L_o+2L}; P = \frac{L_o-R_oT_S}{L_o}$$

$$i_x(k) = \begin{bmatrix} i_A(k) \\ i_B(k) \\ i_C(k) \end{bmatrix} v_{xL}(k) = \begin{bmatrix} v_{LA}(k) \\ v_{LB}(k) \\ v_{LC}(k) \end{bmatrix} v_{xH}(k) = \begin{bmatrix} v_{HA}(k) \\ v_{HB}(k) \\ v_{HC}(k) \end{bmatrix}$$

We see that, to implement FCS-MPC according to (14), we must measure the current $i_x(t)$ and the values $v_{Hx}(k)$ and $v_{Lx}(k)$ in each branch, then extrapolate them to the values $v_{Hx}(k+1)$ and $v_{Lx}(k+1)$ by Euler's method [23]. The current value in (14) will be optimized by the cost function (15) to determine the switching state suitable for the optimized AC side current. Then the current output of the MMC at the current moment will stick to its reference value.

$$J_x = \left|i_{x\_ref}(k+1) - i_x(k+1)\right| \quad (15)$$

Where $i_{x\text{-}ref}$ is the reference of phase's current and $i_x(t+T_s)$ obtained from (14) is the next-step predicted current. The sample period is small enough to $i_{x\_ref}(k+1) \approx i_{x\_ref}(k)$, and (15) rewrites as (16).

$$J_x = \left|i_{x\_ref}(k) - i_x(k+1)\right| \quad (16)$$

In theory, the minimum value of the cost function (16) should be 0. However, in practice, this value is only approximately 0 and is used to select the switching state of the MMC to generate the desired AC current, which is the best possible value of the control objective. This process is repeated many times during the operation of the MMC and is described by the algorithm flowchart as shown in Figure 6.

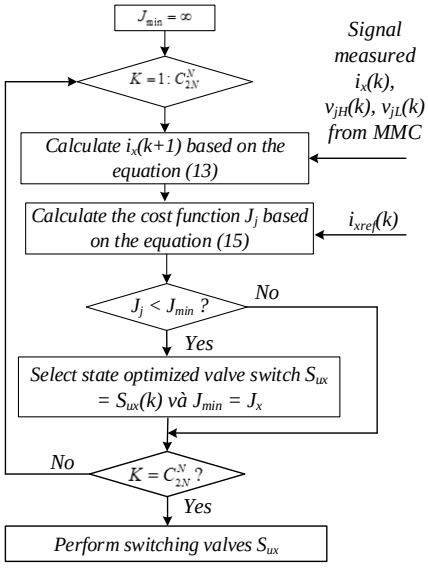

Figure 6. Flowchart of the MPC algorithm to apply to MMC

3.3. Control structure of D-STATCOM system

Since the D-STATCOM system only compensates reactive power, in this control model, active power will not be exchanged with the grid and will always be controlled to 0. Therefore, in the D-STATCOM control system, the control circuit is only designed to generate or absorb reactive power to exchange with the grid [24]. This process will be done by comparing the MMC output voltage value and the grid voltage according to (17).

$$V = V_{ref} + X_S I \quad (17)$$

Here V is measured from the system to compare with its reference value V_{ref}, Xs is the total impedance of the system. The reactive current I is always adjusted within the range (- I_{Max}, I_{Max}). If $V < V_{ref}$, the controller will increase the voltage V to the value V_{ref}, and if $V > V_{ref}$, the controller will decrease the voltage V to the value V_{ref}. The ultimate goal of these two cases is to ensure that the value V is equal to V_{ref} and is shown as shown in the Figure 7 [24].

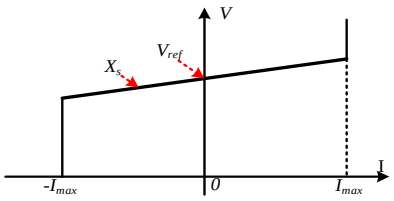

Figure 7. V-I characteristics of D-STATCOM

This makes the reactive power at the grid node always maintained at the desired value. Therefore, to design a controller to compensate for reactive power, it is necessary to design a DC voltage controller [25]. From the D-STATCOM system in Figure 4, we can deduce the relationship between the DC voltage and the AC power in the form of (18) and (19).

$$V_{DC}^2 C_{DC} = \frac{3}{2} v_d i_d = P \quad (18)$$

$$i_d^{ref} = \frac{3v_d}{2V_{DC}} \frac{1}{sC_{DC}} V_{DC}^{ref} \quad (19)$$

The control system of D-STATCOM is designed based on the MMC converter shown in Figure 8, which consists of two control loops to control the stable DC voltage and a control loop to control the reactive power exchanged with the grid according to (19). The FCS-MPC control stage is used in this model to replace the pulse modulation stages.

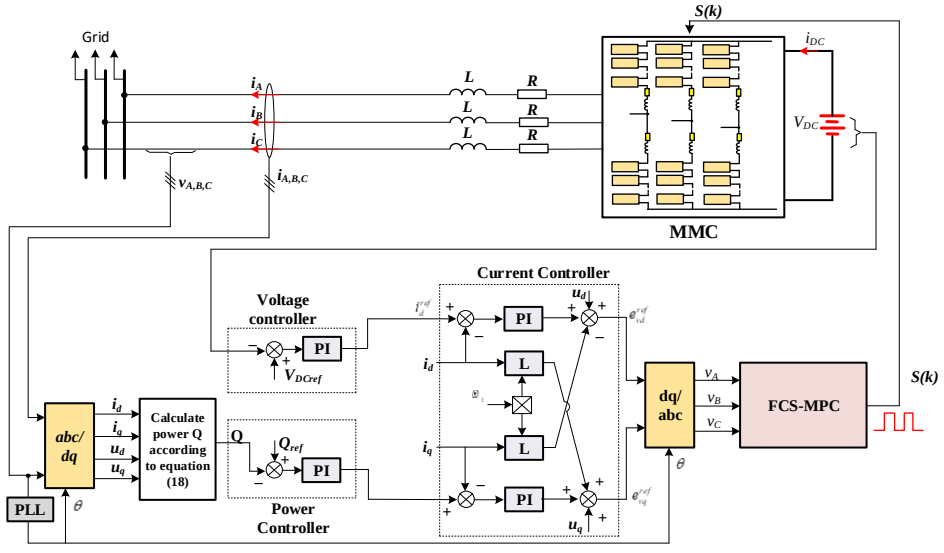

Figure 8. Structure diagram of the D-STATCOM control system based on the MMC controller

4. SIMULATION AND RESULTS

To verify the effectiveness of the predictive controller with the structure as shown in Figure 4. In this section, simulation will be performed by Matlab/Simulink software. The simulation parameters are shown in Table 1. The D-STATCOM system with a maximum power of 3 MVAr connected to the 22 kV

distribution grid will be simulated with scenarios of changing the reactive power amount set over time. The reactive power required from D-STATCOM during the simulation will change according to the scenario as shown in Table 2.

Table 1. Simulation parameters of the system

Parameter	Symbol	Value	Unit
Number of SM per branch	N	10	*SM*
DC voltage of MMC	V_{DC}	10	*kV*
Inductance of the branch	L_o	0.2	*mH*
Power D-STATCOM	S_n	3	*MW*
Ratio of Transformer		5/22 kV	
Resistance of the transformer	R	0.017	Ω
Inductance of the transformer	L	2.1	*mH*
Frequency of grid voltage	f	50	*Hz*
Voltage of distribution grid	V_s	22	*kV*
Sampling cycle	T_s	10^{-5}	*s*

Table 2. Reactive power requirement from D-STATCOM over time

Time	Requirement Q (kVAr)
0-0.25	-1 kVAr
0.25-0.5	-2 kVAr
0.5-0.75	-3 kVAr
0.75-1	3 kVAr

Figures 9 and 10 show the reactive power and active power of the D-STATCOM system. The system only exchanges reactive power without exchanging active power with the grid, so the value of P is always kept at 0. The results show that the reactive power of D-STATCOM always follows the set value with a transition time of only about 0.05 seconds. Thus, the system can well meet the needs of absorbing or generating reactive power.

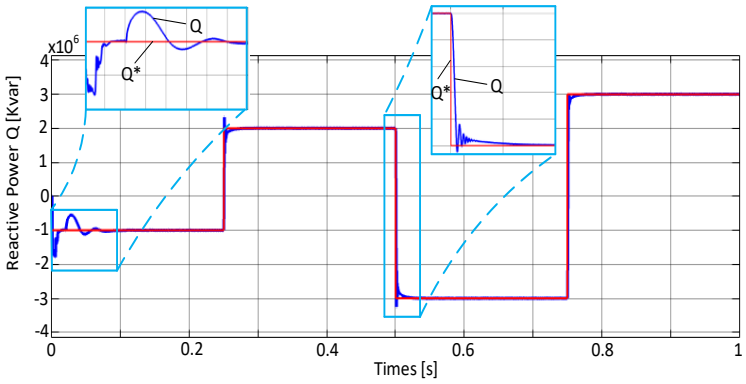

Figure 9. Reactive power of D-STATCOM-MMC exchanged with the grid

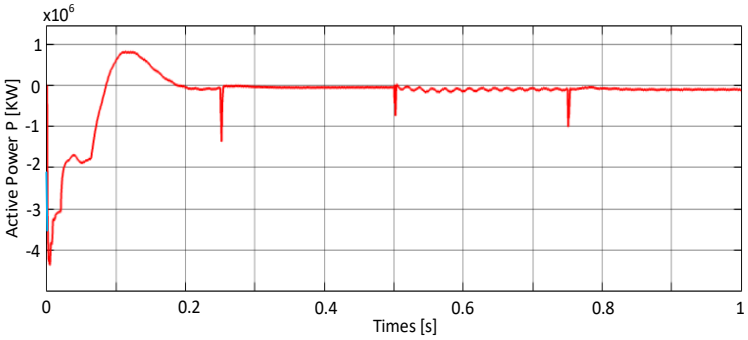

Figure 10. Active power of D-STATCOM-MMC exchanged with the grid

The output current of D-STATCOM in Figure 11 has a pure sinusoidal shape and varies according to the amount of reactive power required by the system. The value of the current always closely follows the set value received from the outer loop control circuit. Figure 12 shows THD index of the current in steady state is only 0.46%, ensuring the allowable harmonic quality indicators.

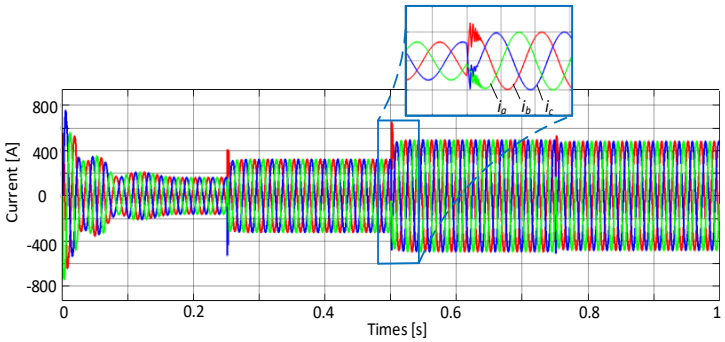

Figure 11. Output current of D-STATCOM

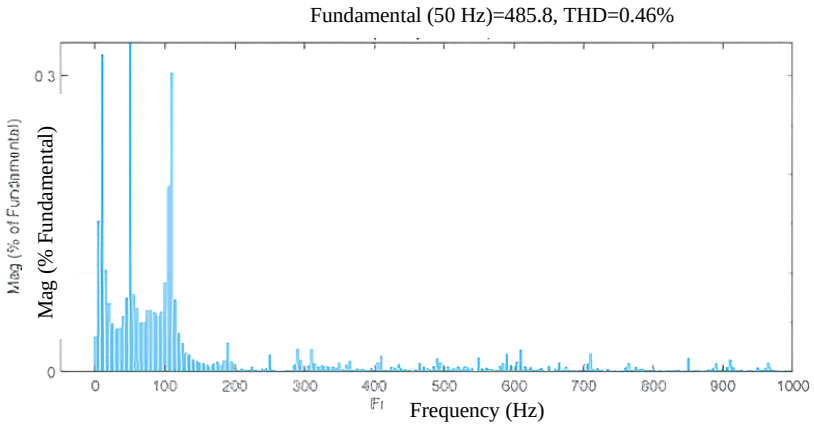

Figure 12. THD index of D-STATCOM output current

Phase A voltage on the AC side of the MMC is shown in Figure 13. The voltage of phase A of MMC is step-shaped, and the value also changes according to the reactive power requirement of D-STATCOM. When the voltage value reaches the maximum of 10000 V, the number of counted voltage steps is 11 levels, which is similar to the theory of the MPC control algorithm in Figure 8. From the results of AC current and voltage, it shows that, with the proposed control strategy, the current and voltage always achieve stable values when the system is working. When changing the set value of AC current and voltage, the controller reacts immediately with the transient exceeding the rated value of about 25% in a very short period of time, about 10^{-5} seconds. After that, the amplitude of current and voltage continues to operate stably according to the system's requirements. This is due to the harmonious combination of PI and MPC control methods, which both ensure fast action and limit transients to the lowest level.

Figure 14 shows the voltage of the upper and lower branch capacitors in phase A of the MMC. The capacitor voltage is initialized at 500 V. After 0.2 seconds, the capacitor voltage fluctuates around 1000V. The maximum pulse is around 130 V (13%). Figure 15 shows the voltage at the node connected to D-STATCOM changes according to the simulation scenarios in Table 2. This proves the ability to regulate the voltage at the power system node of the system. Figure 16 shows the current at the power system node connected to D-STATCOM-MMC. This result shows that the current operates stably according to the amount of reactive power required at the node of the power system.

From the results of current and voltage, when compared with the results published in the documents [9], [12] shows that the response speed of this method is better when paying attention to the power response, as shown in Figure 9, and the immediate grid voltage response, as shown in Figure 15. In addition, the THD value of the D-STATCOM output current has a very low value, showing the outstanding advantages in the quality of system operation compared to traditional.

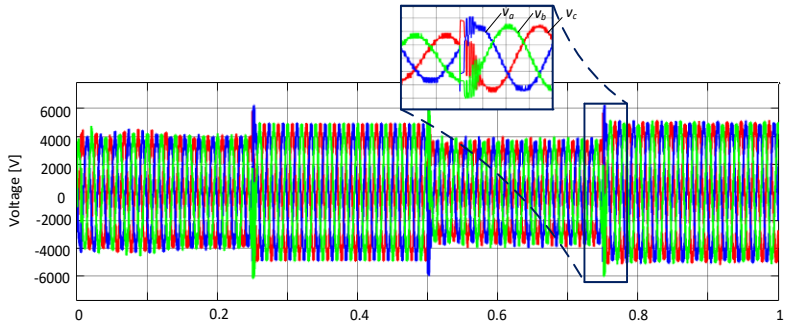

Figure 13. Phase A voltage on the AC side of the MMC

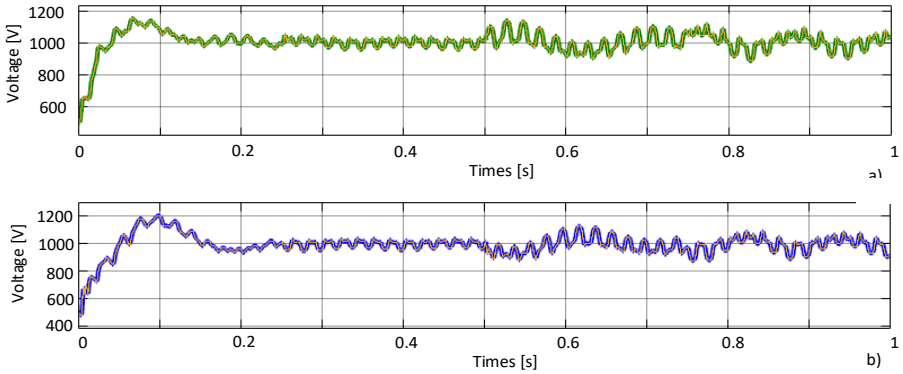

Figure 14. Capacitor voltage of the upper and lower branches of the MMC

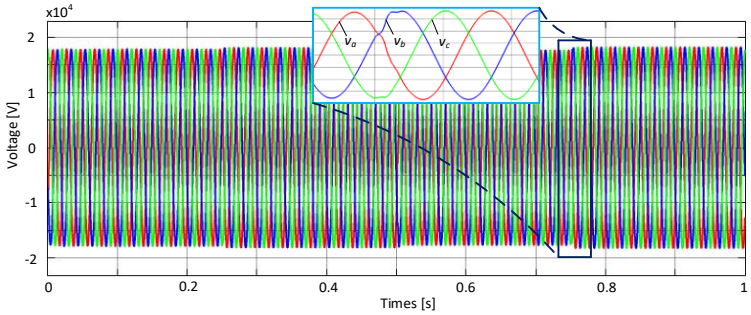

Figure 15. Voltage at the power system node connected to D-STATCOM

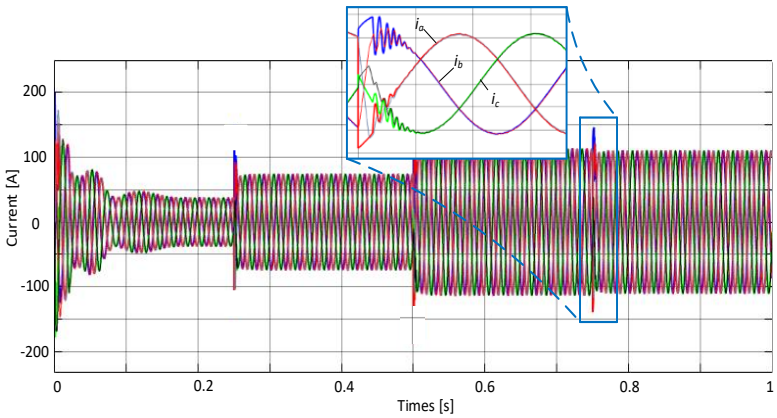

Figure 16. Current at the power system node connected to D-STATCOM

5. CONCLUSION

This paper presents the structure and operating principle of the D-STATCOM reactive power compensation device based on the MMC converter, thereby applying the FCS-MPC control algorithm combined with the PI controller to create control loops to achieve the set goals of reactive power compensation as well as ensure the quality of current and voltage at the nodes of the power system. The simulation results have shown that the application of the FCS-MPC predictive control method for the D-STATCOM compensation device based on the MMC is completely suitable. The system has an output that closely follows the set value, meeting the needs of generating or absorbing CSPK. The current and voltage values all satisfy the quality requirements. This proves that the FCS-MPC predictive controller does a very good job of controlling the output current, the PI has a quick impact, creating accurate set signals for the current loop. The results of this paper are the basic foundation for developing a reactive power compensation product idea for medium voltage power system to provide good quality power to the loads, these results can also be proposed for the development of D-STATCOM devices with FACTS devices in power systems. Additionally, these results can be the basis for demonstration on hardware systems in the laboratory or in real-time feasibility. However, this method also has the disadvantage of requiring a powerful microprocessor to meet the calculation speed of the proposed control algorithm.

FUNDING INFORMATION

This research received no specific grant from any funding agency in the public, commercial, or not-for-profit sectors.

AUTHOR CONTRIBUTIONS STATEMENT

This journal uses the Contributor Roles Taxonomy (CRediT) to recognize individual author contributions, reduce authorship disputes, and facilitate collaboration.

Name of Author	C	M	So	Va	Fo	I	R	D	O	E	Vi	Su	P	Fu
Pham Viet Phuong	✓			✓	✓	✓				✓		✓	✓	✓
Le Hoai Nam		✓	✓				✓	✓	✓		✓	✓		
Pham Chi Hieu		✓			✓	✓		✓	✓	✓	✓			
Tran Hung Cuong	✓		✓	✓	✓		✓		✓	✓			✓	

C : **C**onceptualization
M : **M**ethodology
So : **So**ftware
Va : **Va**lidation
Fo : **Fo**rmal analysis
I : **I**nvestigation
R : **R**esources
D : **D**ata Curation
O : Writing - **O**riginal Draft
E : Writing - Review & **E**diting
Vi : **Vi**sualization
Su : **Su**pervision
P : **P**roject administration
Fu : **Fu**nding acquisition

CONFLICT OF INTEREST STATEMENT

The authors certify that there are no funding involved.

DATA AVAILABILITY

The data that support the findings of this study are available from the corresponding author, [THC], upon reasonable request.

REFERENCES

[1] R. Adware and V. Chandrakar, "A hybrid STATCOM approach to enhance the grid power quality associated with a wind farm," *Engineering, Technology & Applied Science Research*, vol. 13, no. 4, pp. 11426–11431, Aug. 2023, doi: 10.48084/etasr.6125.

[2] O. B. Hadj Brahim Kechiche and M. Mallat, "Modeling and control of a grid-connected photovoltaic system," in *2023 IEEE International Conference on Artificial Intelligence & Green Energy (ICAIGE)*, Oct. 2023, pp. 1–6. doi: 10.1109/ICAIGE58321.2023.10346485.

[3] M. Biswas, S. P. Biswas, S. Mondal, S. S. Haque, S. Hossain, and N. I. Nahin, "A switched-capacitor multilevel transformerless PV inverter with MPC for grid integration," in *2023 10th IEEE International Conference on Power Systems (ICPS)*, Dec. 2023, pp. 1–6. doi: 10.1109/ICPS60393.2023.10429008.

[4] X. Guo *et al.*, "Leakage current suppression of three-phase flying capacitor PV inverter with new carrier modulation and logic function," *IEEE Transactions on Power Electronics*, vol. 33, no. 3, pp. 2127–2135, Mar. 2018, doi: 10.1109/TPEL.2017.2692753.

[5] I. V. Nemoianu, M. Iuliana Dascalu, V. Manescu, G. Paltanea, and R. M. Ciuceanu, "In-deep first assessment of the influence of nonlinear elements in three-phase networks with neutral," in *2019 11th International Symposium on Advanced Topics in Electrical Engineering (ATEE)*, Mar. 2019, pp. 1–6. doi: 10.1109/ATEE.2019.8725000.

[6] O. D. Montoya, C. A. Ramírez-Vanegas, and J. R. González-Granada, "Dynamic active and reactive power compensation in distribution networks using PV-STATCOMs: a tutorial using the Julia software," *Results in Engineering*, vol. 21, p. 101876, Mar. 2024, doi: 10.1016/j.rineng.2024.101876.
[7] H. Bizhani, F. Rezayof Tatari, and G. Iwanski, "Active and reactive power management of hybrid energy systems for reactive power support in distribution network," in *2024 IEEE 15th International Symposium on Power Electronics for Distributed Generation Systems (PEDG)*, Jun. 2024, pp. 1–6. doi: 10.1109/PEDG61800.2024.10667362.
[8] M. Benidris and J. Mitra, "Reliability and sensitivity analysis of composite power systems considering voltage and reactive power constraints," *IET Generation, Transmission and Distribution*, vol. 9, no. 12, pp. 1245–1253, 2015, doi: 10.1049/iet-gtd.2014.0938.
[9] S. H. Eisa Osman, G. K. Irungu, and D. K. Murage, "Application of FVSI, Lmn and CPF techniques for proper positioning of FACTS devices and SCIG wind turbine integrated to a distributed network for voltage stability enhancement," *Engineering, Technology & Applied Science Research*, vol. 9, no. 5, pp. 4824–4829, Oct. 2019, doi: 10.48084/etasr.3101.
[10] F. A. Abdulmunem and A. M. Obais, "Design of a continuously and linearly controlled VSI-based STATCOM for load current balancing purposes," *International Journal of Power Electronics and Drive Systems (IJPEDS)*, vol. 12, no. 1, p. 183, Mar. 2021, doi: 10.11591/ijpeds.v12.i1.pp183-198.
[11] J.F. Gómez-González, D. Cañadillas-Ramallo, B. González-Díaz, J.A. Méndez-Pérez, J. Rodríguez, and R. Guerrero-Lemus, "Reactive power management in photovoltaic installations connected to low-voltage grids to avoid active power curtailment.," *Renewable Energy and Power Quality Journal*, vol. 1, no. 16, pp. 1–11, Jan. 2018, doi: 10.24084/repqj16.003.
[12] T. Ahmed, A. Waqar, Essam A. Al-Ammar, Wonsuk Ko, Yongki Kim, and Muhammad Aamir, "Energy management of a battery storage and D-STATCOM integrated power system using fractional order sliding mode control," *CSEE Journal of Power and Energy Systems*, vol. 7, no. 5, pp. 996–1010, 2021, doi: 10.17775/CSEEJPES.2020.02530.
[13] R. Pandey, R. N. Tripathi, and T. Hanamoto, "Multiband HCC for cascaded H-bridge multilevel inverter based DSTATCOM," in *2016 IEEE 11th Conference on Industrial Electronics and Applications (ICIEA)*, Jun. 2016, pp. 607–612. doi: 10.1109/ICIEA.2016.7603656.
[14] W. Qin, P. Wang, X. Han, and X. Du, "Reactive power aspects in reliability assessment of power systems," *IEEE Transactions on Power Systems*, vol. 26, no. 1, pp. 85–92, Feb. 2011, doi: 10.1109/TPWRS.2010.2050788.
[15] W. Rohouma, R. S. Balog, A. A. Peerzada, and M. M. Begovic, "Capacitor-less D-STATCOM for reactive power compensation," in *2018 IEEE 12th International Conference on Compatibility, Power Electronics and Power Engineering (CPE-POWERENG 2018)*, Apr. 2018, pp. 1–6. doi: 10.1109/CPE.2018.8372590.
[16] G. Gupta, W. Fritz, and M. T. E. Kahn, "A comprehensive review of DSTATCOM: Control and compensation strategies," *International Journal of Applied Engineering Research*, vol. 12, no. 12, pp. 3387–3393, 2017.
[17] C. Kumar and M. K. Mishra, "Energy conservation and power quality improvement with voltage controlled DSTATCOM," in *2013 Annual IEEE India Conference (INDICON)*, Dec. 2013, pp. 1–6. doi: 10.1109/INDCON.2013.6726134.
[18] S. N. Duarte, P. G. Barbosa, and E. Kabalcı, "STATCOM and DSTATCOM with modular multilevel converters," in *Multilevel Inverters*, Elsevier, 2021, pp. 209–248. doi: 10.1016/B978-0-323-90217-5.00008-3.
[19] Y. Tian, H. R. Wickramasinghe, Z. Li, J. Pou, and G. Konstantinou, "Review, classification and loss comparison of modular multilevel converter submodules for HVDC applications," *Energies*, vol. 15, no. 6, p. 1985, Mar. 2022, doi: 10.3390/en15061985.
[20] M. A. Perez, S. Bernet, J. Rodriguez, S. Kouro, and R. Lizana, "Circuit topologies, modeling, control schemes, and applications of modular multilevel converters," *IEEE Transactions on Power Electronics*, vol. 30, no. 1, pp. 4–17, Jan. 2015, doi: 10.1109/TPEL.2014.2310127.
[21] Q. Yang, H. Pourgharibshahi, R. B. Gonzatti, S. Martin, H. Li, and F. Peng, "Modular multilevel converter with minimum arm inductance and automatic sub-module voltage balance - y-matrix modulation and its theoretical proof of the automatic voltage balance," in *2020 IEEE Applied Power Electronics Conference and Exposition (APEC)*, Mar. 2020, pp. 2417–2422. doi: 10.1109/APEC39645.2020.9124457.
[22] R. Picas, J. Pou, S. Ceballos, J. Zaragoza, G. Konstantinou, and V. G. Agelidis, "Optimal injection of harmonics in circulating currents of modular multilevel converters for capacitor voltage ripple minimization," in *2013 IEEE ECCE Asia Downunder*, Jun. 2013, pp. 318–324. doi: 10.1109/ECCE-Asia.2013.6579115.
[23] X. Gao, W. Tian, Z. Zhang, and R. Kennel, "Model predictive control with extrapolation strategy for the arm current commutation control of modular multilevel converter operating in quasi two-level mode," in *2019 10th International Conference on Power Electronics and ECCE Asia (ICPE 2019 - ECCE Asia)*, 2019, pp. 1–6. doi: 10.23919/ICPE2019-ECCEAsia42246.2019.8797192.
[24] Z. Gong, P. Dai, X. Yuan, X. Wu, and G. Guo, "Design and experimental evaluation of fast model predictive control for modular multilevel converters," *IEEE Transactions on Industrial Electronics*, vol. 63, no. 6, pp. 3845–3856, Jun. 2016, doi: 10.1109/TIE.2015.2497254.
[25] V. H. Nguyen, H. Nguyen, M. T. Cao, and K. H. Le, "Performance comparison between PSO and GA in improving dynamic voltage stability in ANFIS controllers for STATCOM," *Engineering, Technology & Applied Science Research*, vol. 9, no. 6, pp. 4863–4869, Dec. 2019, doi: 10.48084/etasr.3032.

BIOGRAPHIES OF AUTHORS

Pham Viet Phuong Pham Viet Phuong was born in Hanoi, Vietnam, on December 24th, 1980. He received the B.S. degree in industrial automation from Hanoi University of Science and Technology, Hanoi, Vietnam, in 2003, the M.S., and Ph.D. degrees in electrical engineering from Tokyo Institute of Technology, Tokyo, Japan, in 2006 and 2009, respectively. Since 2004, he has been a lecturer at the Department of Automation Engineering, School of Electrical and Electronic Engineering, Hanoi University of Science and Technology. His research interests consist of large-capacity power electronics converters, application of power electronics for power systems, and high-power AC motor drives. He can be contacted at email: phuong.phamviet@hust.edu.vn.

Le Hoai Nam received the B.Sc. degree in control and automation engineering from Hanoi University of Science and Technology, Hanoi, Vietnam, in 2024. He is currently studying M.Sc. in Control and Automation Engineering at Hanoi University of Science and Technology, Hanoi, Vietnam. His research interests consist of large-capacity power electronics converters and the application of power electronics for power systems. He can be contacted at email: namlee3102@gmail.com.

Pham Chi Hieu received the B.Sc. degree in control and automation engineering from Hanoi University of Science and Technology, Hanoi, Vietnam, in 2024. He is currently studying M.Sc. in Control and Automation Engineering at Hanoi University of Science and Technology, Hanoi, Vietnam. His research interests consist of large-capacity power electronics converters and the application of power electronics for power systems. He can be contacted at email: chihieu.hust@gmail.com.

Tran Hung Cuong received his Engineer (2010). M.Sc. (2013) degree in industrial automation engineering from Hanoi University of Science and Technology, and completed a Ph.D. degree in 2020 from Hanoi University of Science (HUST). Now, he is a lecturer of Faculty of Electrical and Electronic Engineering, Phenikaa University (PKA). His current interests include power electronic converters, electric motor drives, converting electricity from renewable energy sources to the grid, and energy-saving solutions applied for grid and transportation. He can be contacted at email: cuong.tranhung@phenikaa-uni.edu.vn.